Theoretical calculation methods of stable bearing capacity for thin-walled shells with corrosion and variable temperature

Meccanica
https://doi.org/10.1007/s11012-024-01811-4

Theoretical calculation methods of stable bearing capacity for thin-walled shells with corrosion and variable temperature

Cheng Huijuan Liu · Giuseppe Lacidogna

Received: 4 September 2023 / Accepted: 19 April 2024

Abstract Thin-wall shells (steel plates, steel cylindrical shells, steel spherical shells, etc.) are widely used in many engineering fields such as construction, machinery, chemical industry, navigation, and aviation because of their light weight and high strength. Their failure modes under static pressure or impact dynamic load are mostly buckling instability, and the failure is very sudden, often causing structural failure or even catastrophic accidents without obvious symptoms. In this framework, the significance of this paper is that it considers the influence of external environment corrosion on steel shells' bearing capacity using plate and shell classical stability theory, and investigates the stable bearing capacity of thin-wall steel shells in view of corrosion impact. By this approach, a theoretical calculating method for the time-varying stable bearing capacity of plate and shell thin-walled steel members under the simultaneous action of corrosion and temperature changes is obtained, providing a useful theory for complex engineering practices such as corrosion and temperature changes, including fire actions. Noted that for this method with no analytical solution found, its numerical solutions are given in the appendixes.

Keywords Corrosion · Variable temperature · Fire · Thin-walled shell · Stable bearing capacity

1 Introduction

Thin shell structures (thin plates, thin cylindrical shells, thin spherical shells, etc.) often work in environments with corrosion a0nd temperature changes. According to relevant research, most of their failure problems are controlled by stability. The ultimate goal of this topic is to find the exact solution for the stability performance of shells in this specific environment. From an electrochemical perspective on metals, the paper examines the corrosion process as a time-varying dissolution [1], assuming uniform corrosion across the cross-section [1, 2]. This process not only results in a reduction in shell thickness (which subsequently alters the corrosion rate due to geometric changes) but also typically involves the displacement of the shell boundary (e.g., spherical shell).

In this scenario, it is noted that this uniform dissolution differs from those typically categorized as geometric defects [Liu Response Surface Method] in corrosion. As a result, methodologies based on geometric defect foundations like the Koiter method [3] and perturbation method [4] are deemed unsuitable despite their precision goals. Similarly, it is distinct

C. H. Liu
Department of Mathematics, Aberystwyth University, Aberystwyth, Ceredigion, Wales SY23 3BZ, UK

G. Lacidogna (✉)
Department of Structural, Geotechnical and Building Engineering, Politecnico di Torino, 10129 Turin, Italy
e-mail: giuseppe.lacidogna@polito.it

Published online: 02 September 2024

from random or pitting corrosion defects, making high-energy solid modeling FEM [5] and multi-scale phase-field methods [6] currently inappropriate for directly addressing stability performance (as they are more suited for local cracks or ductility). Additionally, practical approaches like Hutchinson's knock-down factors [7] and NASA's reliability-based analysis [8] are found to be ill-suited for this case, primarily reliant on experiments and empirical data. As a result, the authors of this paper have chosen to employ an analytical theoretical approach [9, 10], focusing on classical theory, over other methods.

Actually, for their stable (unstable) behavior at this time, classical thin-walled shell theories, e.g., small or large deflection theories, can no longer be used directly. Gutman [1, 2, 11] proposed a series of calculation methods for cylindrical shells and spherical shells, mainly in corrosive environments. When dealing with temperature, he does not consider the temperature stress, but only the influence of temperature on the corrosion rate. Lacidogna also mentioned the problem of spherical shell stability after corrosion in literature [12]. But it focuses on the estimation of the stable bearing capacity based on the non-destructive testing data of the shell, and does not discuss the temperature stress in depth. Pronina in the literature [13, 14] took the spherical shell as an example, considered the influence of corrosion and temperature stress, and gave its stable bearing capacity calculation equation, and obtained a segmented analytical solution. However, as for the corrosion kinetic equation it uses comes from Gutman's metal immersion corrosion experiments and has not been verified to be applicable to the type of air corrosion. Also, during the derivation, it doesn't mention constraints (eg: elastic constraints). Although, this has little effect on spherical shells, which are usually considered free constraints. But once it is applied to cylindrical shells or other flat shells, the deficiency will appear. Because cylindrical shells or plate shells often have different levels of restraint at the ends. More importantly, in practice, temperature also changes the physical properties of the shell, such as elastic modulus, yield strength, and possibly even its mode of failure (eg, stability control or strength control). And those things should be discussed. However, research on this type of content has yet to be found.

Among the factors that cause temperature changes, such as: temperature difference between day and night, seasonal temperature difference and fire, fire is more harmful. Therefore, as a special kind of variable temperature environment, its influence on the stability of corroded thin shells should also be discussed. In fact, no relevant research has been found so far.

In this regard, in order to obtain a better and applicable calculation method for thin shells in corrosive and variable temperature environments, this paper starts from the theory of small deflection and large deflection of classical plate shells (in the range of thin walls), and establishes a more general corrosion kinetic model, discusses the post-corrosion stable bearing capacity of thin shells, and establishes calculation methods for them. Then, on this basis, considering the influence of variable temperature on the physical properties of steel and the influence of different levels of constraints on the temperature stress caused by variable temperature, the calculation equation for the stable bearing capacity of thin shells after variable temperature corrosion is established. Finally, aiming at a special and dangerous variable temperature environment—fire, a calculation method for the stable bearing capacity of the corroded thin shell is proposed by introducing the fire variable temperature control curve.

It should be noted that, for the proposed calculation methods, this paper gives priority to finding their analytical solutions. If they are not found or they do not exist, this paper will use numerical methods to solve and verify with examples. It will be noted that some of these results are given in the appendix. The purpose of this is to keep the text flowing, reasonable in length and readable.

2 Problem description

2.1 Objectives of the research

Our purpose is to study the calculation method of the stable bearing capacity of common thin shells (plates, cylindrical shells and spherical shells, shown in Fig. 1) in corrosion and variable temperature environments in the elastic range, and give their possible analytical or numerical solutions.

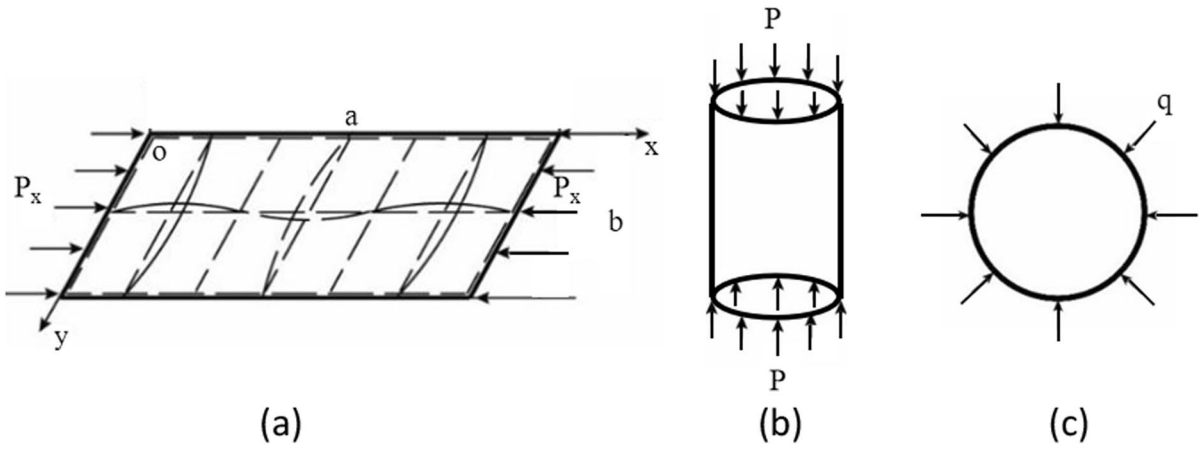

Fig. 1 Thin-wall shells: plates, cylindrical shells, spherical shells. **a** A rectangular plate simply supported on all four sides and uniformly compressed in one direction: with dimensions of length, width, and height a, b, h, respectively, experiencing a distributed pressure of unit length p_x in the x-direction. **b** A cylindrical shell uniformly compressed along its axis: assuming simply supported ends, with radius r, thickness h, and length *L*, experiencing uniform axial pressure p at both ends. The relationship between p and the axial force *N* is given by: $p = N/(2\pi r)$. **c** A spherical shell subjected to uniform external pressure q

2.2 Stability theory under known ideal environment

This paper begins by examining the stability theories of small deflection and large deflection. Their conclusions on the critical stress formulae are illustrated in Eqs. (1)–(21), with a detailed derivation process provided in reference [15]. And only essential results and key steps are presented here.

2.2.1 Plate

The discussion on plates is prioritized due to the plate being a unique type of shell. There are two types of buckling that can occur in plates: small deflection buckling and large deflection buckling. Small deflection buckling involves calculating critical loads for the linear elastic stability theory of thin plates using static equilibrium and energy methods, as demonstrated by [9] and [10]. Interestingly, when a plate reaches its critical load, it may not immediately lose its load-bearing capacity. Instead, it can continue to support the load, a phenomenon known as delayed buckling or post-buckling strength of the plate. This enhanced load-bearing capacity is a result of the plate undergoing large deflection deformation (finite deformation). To analyze the characteristics of delayed buckling, one must employ the theory of large deflection of plates. For instance, researchers often utilize a square plate with four sides simply supported and subjected to uniformly distributed axial pressure N_x (as depicted in Fig. 1a) to investigate stable calculation methods incorporating post-buckling behavior, such as the Worthington method. The subsequent derivation outcomes from these analyses are as follows.

Small deflection buckling:

$$\sigma_{x,cr}(t) = \frac{k\pi^2 E \cdot h^2(t)}{12(1-\mu^2)b^2}, \tag{1}$$

$$p_{x,cr}(t) = \sigma_{x,cr}(t) \cdot h(t) = \frac{k\pi^2 E \cdot h^3(t)}{12(1-\mu^2)b^2}, \tag{2}$$

Large deflection buckling:

$$\sigma_{xa} = \frac{4\pi^2 D}{hb^2} + \frac{E\pi^2 f^2}{8b^2} = \sigma_{cr} + \frac{E\pi^2 f^2}{8b^2} \tag{3}$$

where, σ_{xa} is the average value of the stress at the edge under loading; σ_{cr} is the critical stress of a simply supported rectangular plate; f is the deflection of the plate due to buckling; b is the length of the loaded edge of the plate; D is the flexural rigidity of the plate.

The ultimate load of the plate is:

$$P_u = b_e h \sigma_s, \tag{4}$$

where, P_u is the ultimate load of the plate; b_e is the effective width of the plate; h is the thickness of the plate; σ_s and is the yield strength of the plate.

Regarding b_e the calculation of, it is suggested to take for a simply supported plate:

$$b_e = b\sqrt{\frac{\sigma_{cr}}{\sigma_s}} \tag{5}$$

where, b_e is effective width; σ_{cr} is the critical stress of a four-sided simply supported plate; σ_s is yield strength.

According to a large number of test results, it is suggested to take:

$$b_e = b\sqrt{\frac{\sigma_{cr}}{\sigma_s}}\left(1 - 0.25\sqrt{\frac{\sigma_{cr}}{\sigma_s}}\right) \tag{6}$$

where, b_e is effective width; σ_{cr} is the critical stress of a four-sided simply supported plate; σ_s is yield strength.

In view of the above-mentioned many empirical parameters for the large deflection of the plate, only its small deflection results are adopted in the subsequent equation derivation in this paper.

2.2.2 Cylindrical shell

Similar to the plates mentioned above, a cylindrical shell's stability also falls into two types: large deflection and small deflection

$$\begin{cases} \sigma_{cr}(t) = \begin{cases} \frac{E}{\sqrt{3(1-\mu^2)}}\frac{h(t)}{r}, \text{small deflection buckling} \\ \frac{1}{3}\frac{E}{\sqrt{3(1-\mu^2)}}\frac{h(t)}{r}, \text{large deflection buckling} \end{cases} \\ p_{cr}(t) = \sigma_{cr}(t)\cdot h(t) \\ N_{cr}(t) = \sigma_{cr}(t)\cdot 2\pi r\cdot h(t) \\ \sigma_{cr}(t)\mu h(t) p_{cr}(t) N_{cr}(t) \end{cases} \tag{7}$$

where, $\sigma_{cr}(t)$ is the buckling critical stress of cylindrical shell varying with corrosion time; E is modulus of elasticity; μ is elastic modulus and Poisson's ratio of materials; $h(t)$ is wall thickness of cylindrical shell varying with corrosion time; r is radius; $p_{\mathrm{cr}}(t)$ is critical load that varies with time; $N_{\mathrm{cr}}(t)$ is buckling critical axial force varying with corrosion time.

2.2.3 Spherical shell

Similarly, the stability of the ball shell can be classified into two types: large deflection and small deflection.

$$\sigma_{cr}(t) = \begin{cases} \frac{1}{\sqrt{3(1-\mu^2)}}\frac{Eh(t)}{R}, \text{smalldeflection buckling} \\ \frac{1}{4}\cdot\frac{1}{\sqrt{3(1-\mu^2)}}\cdot\frac{Eh(t)}{R}, \text{large deflection buckling} \end{cases} \tag{8}$$

$$q_{cr}(t) = \frac{2ht)}{R}\sigma_{cr}(t) = \begin{cases} \frac{2E}{\sqrt{3(1-\mu^2)}}\frac{h(t)^2}{R^2}, \text{small deflection buckling} \\ \frac{E}{2\sqrt{3(1-\mu^2)}}\frac{h(t)^2}{R^2}, \text{large deflection buckling} \end{cases} \tag{9}$$

where, $h(t)$ expresses wall thickness of spherical shell with corrosion time; $\sigma_{cr}(t)$ expresses the stable bearing capacity of spherical shell varies with corrosion time); $q_{cr}(t)$ expresses critical load of spherical shell with corrosion time).

2.3 Other required unknown conditions or governing equations

From the basic equations of critical stress theory known above (see formulas (1)–(9) in Sect. 2.2), it can be observed that before achieving the goal of this paper, three related sub-problems need to be improved or discussed. Firstly, an applicable dynamic corrosion model; secondly, the performance of steel materials at different temperatures; thirdly, the relationship between temperature stress and constraints; and fourthly, the control equation for the fire temperature curve.

2.3.1 A more general and improved kinetic corrosion model

The current corrosion models mainly come from the fitting of experimental data, one of which comes from the experimental data of air corrosion [16], and its expression is:

$$D = At^n \tag{10}$$

where, D is corrosion depth; A is corrosion rate; t is time (year); n is development trend of corrosion process.

When at natural exposure $\sigma=0$, formula (10) becomes:

$$\frac{dh}{dt} = -v_0 \approx -A \tag{11}$$

We treat it as a reference value (when $\sigma=0$).

The other model obtained from the corrosion experimental data of metals in solution [1], and its expression is:

$$\frac{dh}{dt} = -v_0 exp\frac{V\sigma}{RT} \tag{12}$$

where, v_0 is initial corrosion rate of a metal in a borderless stress state); V is the molar volume of a substance); σ is the absolute value of stress in a metal under unidirectional loading below the elastic limit); R is 8.314 J/(mol·K)(ideal gas constant, which is usually 8.314 J/(mol·K)); T is absolute temperature.

This model can consider the effect of different levels on the corrosion rate. It is easy to see that when at natural exposure $\sigma=0$, formula (12) becomes:

$$\frac{dh}{dt} = -Ant^{n-1} \tag{13}$$

However, the formula (13) deviates greatly from the reference value (10b), and this error reflects that the proof formula (14) is not applicable at $\sigma=0$.

To illustrate this deviation more graphically, we use an example of a naturally exposed board at room temperature. Its physical and geometric parameters are, the wall thickness of the rectangular steel plate is 5 mm, and the material is 1 6 Mn steel. Corrosion occurred in the Qingdao area, corresponding to A = 0.055, n = 0.65. The temperature is 20 °C (i.e. 293 K) at room temperature. According to the power function prediction model (Eq. 10), the relationship of thickness with time can be obtained as: $h = h_0 - 0.055t^{0.65}$. Take the molar volume of the steel $V = 7 \times 10^{-6} m^3/mol$, the gas constant $R = 8.314 J/mol \cdot K = 8.314 N \cdot m/mol \cdot K$, R = 8.314 J/mol·K = 8.314/N m/mol·K, and the temperature T = 293 K, that is, the normal temperature of 20 °C.

We used formula (13) and (11) models respectively to plot the corrosion thickness and time curve of this plate, and the results were shown in Fig. 2. The figure

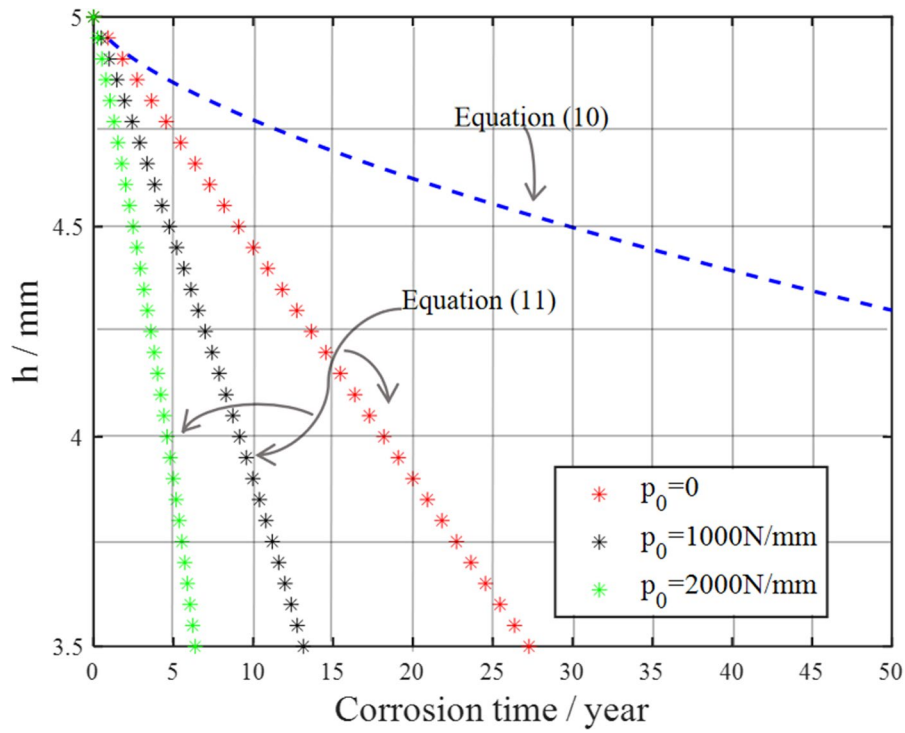

Fig. 2 Variation curve of wall thickness with corrosion time

shows as the two models have different results when there is no stress. The initial pressure on the shell, represented by p_0, remains constant during corrosion, and it is clear that the blue curve (from Eq. (10)) and the other curves (from Eq. (13)) show a significant dispersion.

It can be seen than Fig. 2 vividly shows that we need a new and improved corrosion model to eliminate this difference to obtain a corrosion model that is more general to the environment. In this regard, on the basis of these two models, this paper proposes an improved empirical model, as follows:

$$\frac{dh}{dt} = Ant^{n-1} exp\frac{V\sigma}{RT} \tag{14}$$

where, A is initial corrosion rate); n is development trend of corrosion process; t is exposure time (years); V is the molar volume of a substance; σ is absolute value of stress in a metal under unidirectional loading below the elastic limit; R is ideal gas constant, usually 8.314 J/(mol·K); T is absolute temperature.

This paper uses this new model in Eq. (14) instead of the model shown in Eq. (12) to draw the curves again (firstly shown in Fig. 2), and finds that they (the red stars and the blue line) fit well now shown in Fig. 3. This shows that the improved model can be consistent with the experimental data of the two types of environments at the same time, and it is a more universal model.

2.3.2 *Material properties of structural steel at varying temperatures*

The elastic modulus expression of steel at high temperature is as follows:

$$E(T_s) = \begin{cases} \frac{7T_s - 4780}{6T_s - 4760} E_s, & 20°C \le T_s < 600°C \\ \frac{1000 - T_s}{6T_s - 2800} E_s, & 600°C \le T_s < 1000°C \end{cases} \tag{15}$$

where, T_s is the temperature of steel; $E(T_s)$ is the elastic modulus of steel at high temperature (N/mm^2); E_s is the elastic modulus of steel at normal temperature (N/mm^2); mm^2), it can be taken as 206 Gpa [18] according to the literature [17].

The Eq. [19] for calculating the strength design value of steel at high temperature is as follows:

$$f_T = \eta_{sT} f \tag{16}$$

In the equation,

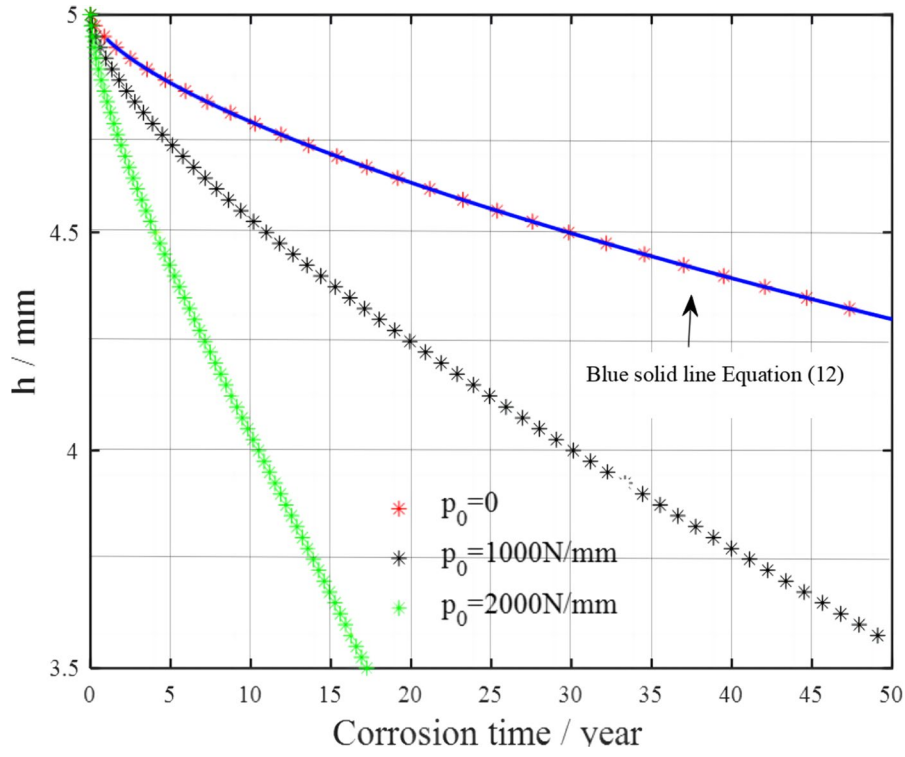

Fig. 3 Wall thickness-corrosion time curve obtained based on the improved corrosion model

$$\eta_{sT}=\begin{cases}1.0\ , & 20^0\mathrm{C}\le T_s\le 300^0\mathrm{C}\\ 1.24\times10^{-8}T_s^3-2.096\times10^{-5}T_s^2+9.288\times10^{-3}T_s-0.2168 & 300\le T_s\le 800^0\mathrm{C}\\ 0.5-T_s/2000, & 800\le T_s\le 1000^0\mathrm{C}\end{cases} \tag{17}$$

where, f_T is the strength design value of the steel at high temperature; f is the strength design value of the steel at room temperature; η_{sT} is the yield strength reduction coefficient of the steel at high temperature; T_s is the temperature of the steel.

It was found that Poisson's ratio is less affected by temperature changes, therefore, in the temperature range discussed in this paper, Poisson's ratio is considered as a constant value.

2.3.3 *Relationship between temperature stress and constraints.*

The constraints discussed in this paper mainly refer to no constraints, elastic constraints and rigid constraints [20]. In this paper, under these three different constraints, the stresses caused by variable temperature are discussed.

Under arbitrary elastic constraints, the temperature stress equation s of plates and cylindrical shells are as follows.

Plate:

$$\sigma_{cr}(t_c,T_s)=\frac{k\pi^2\cdot h^2(t_c)\cdot E(T_s)}{12(1-\mu^2)b^2}-k_r\alpha_T(T_s-T_{s0})E(T_s) \tag{18}$$

Cylindrical shell:

$$\sigma_{cr}(t_c,T_s)=\begin{cases}\frac{h(t_c)}{r}\frac{E(T_s)}{\sqrt{3(1-\mu^2)}}-k_r\alpha_T(T_s-T_{s0})E(T_s)\\ \frac{1}{3}\frac{h(t)}{r}\frac{E(T_s)}{\sqrt{3(1-\mu^2)}}-k_r\alpha_T(T_s-T_{s0})E(T_s)\end{cases} \tag{19}$$

where, $E(T_s)$ is elastic modulus of steel ball shell at corresponding temperature; $\sigma_{cr}(t_c,T_s)$ is the stable bearing capacity of steel ball shell with corrosion time; k_r is constraint degree coefficient; T_0 is initial time temperature; T is the temperature of the current moment; α_T is linear thermal expansion coefficient of material.

The spherical shell is considered free and unconstrained, so its temperature stress is:

$$\sigma_{cr}(t_c,T_s)=\begin{cases}\frac{h(t_c)}{r}\frac{E(T_s)}{\sqrt{3(1-\mu^2)}}\\ \frac{1}{4}\frac{h(t)}{r}\frac{E(T_s)}{\sqrt{3(1-\mu^2)}}\end{cases} \tag{20}$$

$\sigma_{cr}(t_c,T_s)$ is the stable bearing capacity of steel ball shell with corrosion time;$E(T_s)$ is elastic modulus of steel ball at corrosion time; $h(t_c)$ is thickness of the spherical shell changes with the corrosion time. The meanings of other parameters are the same as the preceding ones; thickness of the spherical shell changes with the corrosion time. The meanings of other parameters are the same as the preceding ones.

Their derivation is shown in Appendix A using a cylindrical shell as an example.

2.3.4 *Governing equation of fire temperature curve*

The variable temperature control equation of fire is the temperature control curve of steel members with light fire protection layer under standard fire [21]:

$$T_s=\left(\sqrt{0.044+5.0\times10^{-5}\alpha\frac{F_i}{V}}-0.2\right)t+T_{s0}\ T_s\le 700^{\circ}\mathrm{C} \tag{21}$$

In the equation: t—fire duration (s); T_{s0}—initial temperature of steel member before fire, which can be taken as 20 °C; F_i—fired surface area per unit length of steel member with fire protection (m^2); V—unit length of steel member volume (m^3);α—comprehensive heat transfer coefficient [W/(m^2°C)].

In short, based on the basic Eqs. (1)–(9) mentioned above, as well as the related boundary or control Eqs. (10)–(21), and by using analytical and numerical methods, we will gradually achieve the goal of this paper in three steps: developing a stability calculation method for temperature-corrosion thin-walled shells. The first step involves deriving a stability calculation method for thin shells in a corrosive environment. In the second step, building upon the first one, the temperature factor is introduced to derive a stability calculation method for thin shells under corrosive

temperatures. The third step further incorporates the fire temperature control equation based on the second step to derive a stable calculation method for fire-induced temperature-corrosion shells. The specific key derivation steps for these methods are outlined in Sects. 3, 4, and 5, respectively.

3 Stability calculation method for thin shells in corrosion environment

In this section, we will systematically derive the stability of corroding thin-walled shells (including plates, cylindrical shells, and spherical shells) based on the Eqs. (1)–(14) provided above. We will outline key derivation steps for each type of thin shell and discuss the implications of these calculations.

3.1 Plate

The stress of the plate can be expressed as,

$$\sigma(t) = \frac{p_0}{h(t)}, \tag{22}$$

where, p_0 is the constant load (here is the line load at both ends of the plate); $h(t)$, $\sigma(t)$ is the time-varying thickness and time-varying stress of the plate, respectively. Substituting Eq. (17) into (12) we get:

$$\frac{dh}{dt} = -Ant^{n-1}exp\frac{V\sigma}{RT} = -Ant^{n-1}exp\frac{Vp_0}{RTh}, \tag{23}$$

where, A is initial corrosion rate; n is the development trend of corrosion process; t is exposure time (years); V is the molar volume of a substance; σ is absolute value of stress in a metal under unidirectional loading below the elastic limit; R is the ideal gas constant, usually 8.314 J/(mol·K); T is absolute temperature.

We write Eq. (23) as:

$$-\frac{1}{A}exp(-\frac{Vp_0}{RTh})dh = -nt^{n-1}dt. \tag{24}$$

We integrate it in the range of h_0- h, t_0- t to get:

$$t = [-\frac{1}{A}\int_{h_0}^{h} exp(-\frac{Vp_0}{RTh})dh]^{\frac{1}{n}} \tag{25}$$

Ordering $t = f(h) = [-\frac{1}{A}\int_{h_0}^{h} exp(-\frac{Vp_0}{RTh})dh]^{\frac{1}{n}}$, f expresses the corresponding rule between variable h and variable t.

Since there is a one-to-one correspondence between plate thickness h and corrosion time t, the inverse operation exists: $h = f^{-1}(t)$.

Substituting h into Eq. (25) can obtain the calculation expressions of the buckling critical stress and critical load of the plate:

$$\begin{cases} t = f(h) = [-\frac{1}{A}\int_{h_0}^{h} exp(-\frac{Vp_0}{RTh})dh]^{\frac{1}{n}} \\ h = f^{-1}(t) \\ \sigma_{x,cr}(t) = \frac{k\pi^2 E}{12(1-\mu^2)}\frac{[f^{-1}(t)]^2}{b^2} \\ p_{x,cr}(t) = \sigma_{x,cr}(t)\cdot h(t) = \frac{k\pi^2 E}{12(1-\mu^2)}\frac{[f^{-1}(t)]^3}{b^2} \end{cases} \tag{26}$$

3.2 Cylindrical shells

The stress of the cylindrical shell is expressed as

$$\sigma(t) = \frac{N}{2\pi r\cdot h(t)} \tag{27}$$

Considering Eq. (12), we have

$$\frac{dh}{dt} = -Ant^{n-1}exp\frac{V\sigma}{RT} = -Ant^{n-1}exp\frac{VN}{2\pi rhRT} \tag{28}$$

where, A is initial corrosion rate; n is the development trend of corrosion process; t is exposure time (years); V is the molar volume of a substance; σ is the absolute value of stress in a metal under unidirectional loading below the elastic limit; R is the ideal gas constant, usually 8.314 J/(mol·K); T is absolute temperature.

Integrating it over h_0 to h and 0 to t gives:

$$\int_{h_0}^{h} -\frac{1}{A}exp(-\frac{VN}{2\pi rhRT})dh = \int_{0}^{t} nt^{n-1}dt, \tag{29}$$

After integral operation, we can get:

$$t = [-\frac{1}{A}\int_{h_0}^{h} exp(-\frac{VN}{2\pi rhRT})dh]^{\frac{1}{n}} \tag{30}$$

Let$t = f(h) = [-\frac{1}{A}\int_{h_0}^{h} exp(-\frac{VN}{2\pi rhRT})dh]^{\frac{1}{n}}$, f express the correspondence rule between variable h and variable t, since there is a one-to-one correspondence between plate thickness h and corrosion time t, we have: $h = f^{-1}(t)$.

Putting h into the above equation, the calculation method of critical buckling stress, critical line load and critical axial resultant force of cylindrical shell can be obtained:

$$\begin{cases} t = f(h) = [-\frac{1}{A}\int_{h_0}^{h} exp(-\frac{VN}{2\pi rhRT})dh]^{\frac{1}{n}} \\ h = f^{-1}(t) \\ \sigma_{cr}(t) = \begin{cases} \frac{E}{\sqrt{3(1-\mu^2)}} \cdot \frac{f^{-1}(t)}{r}, small deflection buckling \\ \frac{1}{3} \cdot \frac{E}{\sqrt{3(1-\mu^2)}} \cdot \frac{f^{-1}(t)}{r}, large deflection buckling \end{cases} \\ p_{cr}(t) = h(t) \cdot \sigma_{cr}(t) \\ N_{cr}(t) = 2\pi r \cdot h(t) \cdot \sigma_{cr}(t) \end{cases} \tag{31}$$

Among them, f^{-1} is f the inverse function of the function.

3.3 Spherical shell

The stress of the spherical shell is expressed as

$$\sigma(t) = \frac{qr}{2h(t)}. \tag{32}$$

Considering Eq. (14), we have:

$$\frac{dh}{dt} = -Ant^{n-1}exp\frac{V\sigma}{RT} = -Ant^{n-1}exp\frac{Vqr}{2hRT} \tag{33}$$

where, A is initial corrosion rate; n is the development trend of corrosion process; t is exposure time (year); V is the molar volume of a substance; σ is; R is the ideal gas constant, usually 8.314 J/(mol·K); T is absolute temperature.

It over h_0 to h and t_0 to t:

$$\int_{h_0}^{h} -\frac{1}{A}exp(-\frac{Vqr}{2hRT})dh = \int_{0}^{t} nt^{n-1}dt, \tag{34}$$

Available after operation

$$t = [-\frac{1}{A}\int_{h_0}^{h} exp(-\frac{Vqr}{2hRT})dh]^{\frac{1}{n}} \tag{35}$$

Ordering $t = f(h) = [-\frac{1}{A}\int_{h_0}^{h} exp(-\frac{Vqr}{2hRT})dh]^{\frac{1}{n}}$, f expresses the corresponding rule between variable h and variable t.

Since there is a one-to-one correspondence between plate thickness h and corrosion time t, it can be obtained by inverse calculation $h = f^{-1}(t)$.

Putting h into the above equation, the calculation method of buckling critical stress and critical load can be obtained as follows:

$$\begin{cases} t = f(h) = [-\frac{1}{A}\int_{h_0}^{h} exp(-\frac{Vqr}{2hRT})dh]^{\frac{1}{n}} \\ h = f^{-1}(t) \\ \sigma_{cr}(t) = \begin{cases} \frac{E}{\sqrt{3(1-\mu^2)}} \frac{f^{-1}(t)}{r}, \text{small deflection buckling} \\ \frac{1}{4} \cdot \frac{E}{\sqrt{3(1-\mu^2)}} \cdot \frac{f^{-1}(t)}{r}, \text{large deflection buckling} \end{cases} \\ q_{cr}(t) = \frac{2h(t)\cdot\sigma_{cr}(t)}{r} \end{cases} \tag{36}$$

where, f^{-1} is f the inverse of the function.

4 Calculation method of stable bearing capacity of thin shell under corrosion temperature change

In this section, we can build on the equation derived in Sect. 3, and then continue the derivation by considering the effect of varying temperature (stress) (Eqs. (18)–(20)). Their related results are shown below.

4.1 Plate

Critical stress expression when the loaded edge of the plate is subject to arbitrary elastic constraints is:

$$\begin{cases} \frac{dh}{dt_c} = Ant_c^{n-1}exp\frac{V\sigma}{RT_g} \\ E(T_s) = \frac{7T_s-4780}{6T_s-4760}E_s, 20°C \le T_s < 600°C \\ \sigma_{cr}(t_c, T_s) = \frac{k\pi^2\cdot h^2(t_c)\cdot E(T_s)}{12(1-\mu^2)b^2} - k_r\alpha_T(T_s - T_{s0})E(T_s) \\ p_{cr}(t_c, T_s) = \sigma_{cr}(t_c, T_s) \cdot h(t_c) \end{cases} \tag{37}$$

In the Eq. (37), T_0 represents the temperature at the initial moment, T s represents the temperature of the plate at the current moment, α_T and represents the linear thermal expansion coefficient of the material, $E(T_s)$ represents the elastic modulus of the plate that changes with temperature; $h(t_c)$ Indicates indicates the thickness of the plate that changes with the corrosion time; $\sigma_{cr}(t_c, T_s)$ is the stable bearing capacity of steel ball shell with corrosion time, represents $p_{cr}(t_c, T_s)$ represents the stable bearing capacity of the plate that changes in real time with the corrosion time and temperature; k_r is the constraint coefficient of the loaded

side; k is the critical load coefficient. The remaining parameters have the same meaning as before.

4.2 Cylindrical shell

When the two loaded sides of a cylindrical shell are subjected to arbitrary elastic constraints, its critical stress can be expressed as

$$\begin{cases} \dfrac{dh}{dt_c} = Ant_c^{n-1} \exp \dfrac{V\sigma}{RT_g} \\ E(T_s) = \dfrac{7T_s - 4780}{6T_s - 4760} E_s \ , \ 20°\mathrm{C} \le T_s < 600°\mathrm{C} \\ \sigma_{cr}(t_c, T_s) = \begin{cases} \dfrac{h(t_c)}{R} \dfrac{E(T_s)}{\sqrt{3(1-\mu^2)}} - k_r \alpha_T (T_s - T_{s0}) E(T_s), \ \textit{small deflection buckling} \\ \dfrac{1}{3} \cdot \dfrac{h(t_c)}{R} \dfrac{E(T_s)}{\sqrt{3(1-\mu^2)}} - k_r \alpha_T (T_s - T_{s0}) E(T_s), \ \textit{large deflection buckling} \end{cases} \\ p_{cr}(t_c, T_s) = h(t_c) \cdot \sigma_{cr}(t_c, T_s) \\ N_{cr}(t_c, T_s) = 2\pi r \cdot h(t_c) \cdot \sigma_{cr}(t_c, T_s) \end{cases} \tag{38}$$

In the Eq. (38), T_0 represents the temperature at the initial moment, T_s represents the temperature at the current moment of the cylindrical shell, and α_T represents the linear thermal expansion coefficient of the material, $E(T_s)$ represents the elastic modulus of the cylindrical shell that changes with temperature; $h(t_c)$ represents the thickness of the cylindrical shell that changes with the corrosion time; $\sigma_{cr}(t_c, T_s)$ is the stable bearing capacity of steel ball shell with corrosion time; represents $p_{cr}(t_c, T_s)$ represents the stable bearing capacity of the cylindrical shell that changes in real time with the corrosion time and temperature; is k_r is the constraint coefficient of the loaded side; k is the critical load coefficient. The remaining parameters have the same meaning as before.

4.3 Spherical shell

The spherical shell is considered as a free structure in this paper. Therefore, its thermal deformation is not limited, that is, the temperature stress caused by the temperature change in the spherical shell cannot be considered, but only the change of the elastic modulus caused by the temperature change can be considered. Therefore, its critical stress can be expressed as:

$$\begin{cases} \frac{dh}{dt_c} = Ant_c^{n-1} exp \frac{V\sigma}{RT_g} \\ E(T_s) = \frac{7T_s - 4780}{6T_s - 4760} E_s, 20°C \le T_s < 600°C \\ \sigma_{cr}(t_c, T_s) = \begin{cases} \frac{h(t_c)}{r} \frac{E(T_s)}{\sqrt{3(1-\mu^2)}}, \text{small deflection buckling} \\ \frac{1}{4} \frac{h(t)}{r} \frac{E(T_s)}{\sqrt{3(1-\mu^2)}}, \text{large deflection buckling} \end{cases} \\ q_{cr}(t_c, T_s) = \frac{2 \cdot h(t_c) \cdot \sigma_{cr}(t_c, T_s)}{r} \end{cases} \tag{39}$$

In the Eq. (39), $E(T_s)$ represents the elastic modulus of the steel spherical shell at the corresponding temperature; represents the thickness of the spherical shell $h(t_c)$ that changes with the corrosion time; $h(t_c)$ represents the thickness of the cylindrical shell that changes with the corrosion time; $\sigma_{cr}(t_c, T_s)$ is the stable bearing capacity of steel ball shell with corrosion time; $q_{cr}(t_c, T_s)$ represents the stable bearing capacity of the steel spherical shell that changes with the corrosion time and steel temperature.

5 Calculation method of stable bearing capacity of corroded thin shells under variable temperature in fire

In this section, we further develop the equations from Sect. 4 by including the fire protection curve (Eq. (18)) without considering the change in wall thickness h during the fire exposure. Here, we assume that $h(t_c)=h(t_0)$ since ignition times are generally much shorter than the corrosion period. This assumption enables us to determine the stable bearing capacity of variable temperature corrosion shells under fire conditions. The outcomes for plates, cylindrical shells, and spherical shells are detailed below:

5.1 Plate

The plate behavior under variable temperature in fire is as follows:

$$\begin{cases} T_s = (\sqrt{0.044 + 5.0 \times 10^{-5} \alpha \frac{F_i}{V}} - 0.2)t_s + T_{s0}, T_s \le 700^oC \\ E(T_s) = \frac{7T_s - 4780}{6T_s - 4760} E_s, 20°C \le T_s < 600°C \\ \sigma_{cr}(t_c, T_s) = \frac{k\pi^2 \cdot h^2(t_c) \cdot E(T_s)}{12(1-\mu^2)b^2} - k_r \alpha_T (T_s - T_{s0}) E(T_s), 20°C \le T_s < 600°C \end{cases} \tag{40}$$

where, α_T and represents the linear thermal expansion coefficient of the material, $E(T_s)$ represents the elastic modulus of the plate that changes with temperature; $h(t_c)$ indicates the thickness of the plate that changes with the corrosion time; $\sigma_{cr}(t_c, T_s)$ is the stable bearing capacity of steel ball shell with corrosion time; $p_{cr}(t_c, T_s)$ represents the stable bearing capacity of the plate that changes in real time with the corrosion time and temperature; k_r is the constraint coefficient of the loaded side; k is the critical load coefficient. The remaining parameters have the same meaning as before.

Among them, the third equation can also be written as:

$$\sigma_{cr}(t_c, t_s) = \frac{k\pi^2 \cdot h^2(t_c) \cdot E(t_s)}{12(1-\mu^2)b^2} - k_r \alpha_T (T_s - T_{s0}) E(t_s) \tag{41}$$

5.2 Cylindrical shells

The thin cylindrical shell under variable temperature in fire is as follows:

$$\begin{cases} T_s = (\sqrt{0.044 + 5.0 \times 10^{-5} \alpha \frac{F_i}{V}} - 0.2)t + T_{s0}, T_s \le 700^oC \\ E(T_s) = \frac{7T_s - 4780}{6T_s - 4760} E_s, 20°C \le T_s < 600°C \\ \sigma_{cr}(t_c, T_s) = \frac{1}{3} \cdot \frac{h(t_c)}{R} \frac{E(T_s)}{\sqrt{3(1-\mu^2)}} - k_r \alpha_T (T_s - T_{s0}) E(T_s), 20°C \le T_s < 600°C \end{cases} \tag{42}$$

The third equation can also be written as:

$$\sigma_{cr}(t_c, t_s) = \frac{1}{3} \cdot \frac{h(t_c)}{R} \frac{E(t_s)}{\sqrt{3(1-\mu^2)}} - k_r \alpha_T (T_s - T_{s0}) E(t_s) \tag{43}$$

5.3 Spherical shell

The calculation method of the stable bearing capacity of a thin spherical shell under fire temperature changes is as follows:

$$\begin{cases} T_s = (\sqrt{0.044 + 5.0 \times 10^{-5} \alpha \frac{F_i}{V}} - 0.2) t_s + T_{s0} \quad T_s \le 700^{\circ}C \\ E(T_s) = \frac{7T_s - 4780}{6T_s - 4760} E_s, 20^{\circ}C \le T_s < 600^{\circ}C \\ \sigma_{cr}(t_c, T_s) = \frac{1}{4} \frac{h(t_c)}{r} \frac{E(T_s)}{\sqrt{3(1-\mu^2)}}, 20^{\circ}C \le T_s < 600^{\circ}C \end{cases} \tag{44}$$

The third equation can also be written as:

$$\sigma_{cr}(t_c, t_s) = \frac{1}{4} \frac{h(t_c)}{r} \frac{E(t_s)}{\sqrt{3(1-\mu^2)}} \tag{45}$$

Note: The calculation methods proposed in Sects. 3, 4, and 5 of this paper are difficult to find analytical solutions (mainly because of the exponential part existing in the corrosion kinetic model, the explicit integral result is difficult to obtain in the field of elementary function field). Therefore, a numerical analysis of them is carried out in this paper, and the relevant diagrams and descriptions can be found in Appendix B–J.

6 Conclusion

From an electrochemical perspective, based on the assumption of uniform and time-varying dissolution of visual metal corrosion, we have conducted a solid theoretical derivation work with the goal of stable shell analysis method in a corroded temperature changing environment. In this paper, we have conducted some solid theoretical derivations. A more general corrosion kinetic model is first proposed. Then, based on the model, starting from the basic stability theory, the calculation method of the stable bearing capacity of the thin shell under different corrosion temperature is deduced by combining the temperature stress and the change of steel physical properties under different constraints. Finally, considering the special variable temperature-fire control curve, the calculation method of the stable bearing capacity of the fire variable temperature corroded thin shell is deduced.

Funding Open access funding provided by Politecnico di Torino within the CRUI-CARE Agreement. The sponsorship guaranteed with basic research funds provided by Politecnico di Torino, Italy, for its financial aid in this work is acknowledged.

Declarations

Competing interests The authors declare no conflict of interest.

Appendix A

Stress expressions for cylindrical shells subject to arbitrary elastic constraints

If the two loaded sides of the cylindrical shell are elastically constrained arbitrarily, following [12], the constraint coefficient is defined as kr. Under the action of temperature, the stress–strain relationship in the cylindrical shell is:

$$\sigma_T = \varepsilon_T E(T_s) \tag{46}$$

In the equation, α_T is the temperature stress; $E(T_s)$ is the elastic modulus of ε_T the steel; is the strain (or constraint strain) that produces the temperature stress, and its calculation expression is:

$$\varepsilon_T = \varepsilon_c - \alpha_T \Delta T. \tag{47}$$

In the equation, α_T is the linear expansion coefficient of the material; ΔT is the temperature change; ε_c is the actual strain; $\alpha_T \Delta T$ is the free strain generated when it is not restrained. Substituting Eqs. (47) into (46), we have:

$$\sigma_T = \left(\varepsilon_c - \alpha_T \Delta T\right) E\left(T_s\right). \tag{48}$$

In fact, fixed constraints and free constraints can be seen as the two extremes of elastic constraints. In the fixed constraint state, the actual strain produced by $\varepsilon_c = 0$ the cylindrical shell has the maximum temperature stress$\sigma_T = -E(T_s)\alpha_T \Delta T$; in the free state, the actual strain $\varepsilon_c = \alpha_T \Delta T$ has the minimum temperature stress $\sigma_T = 0$. It can be seen that the temperature stress in the structure is related to the restraint degree of the structure. In order to scientifically describe the relationship between temperature stress and degree of restraint, the restraint coefficient is defined as follows:

$$k_r = 1 - \frac{\varepsilon_c}{\alpha_s \Delta T} \tag{49}$$

It can be known from the above equation: (a) when the structure is in a fixed restraint state, the actual strain $\varepsilon_c = 0$, the restraint coefficient $k_r = 1$; (b) when the structure is in a free state, the actual strain$\varepsilon_c = \alpha_T \Delta T$, the restraint coefficient$k_r = 0$; (c) when When the structure is in any elastic constraint state, the actual strain ε_c is between 0 and$\alpha_T \Delta T$, that is, there is $0 < k_r < 1$.

Substituting (46) into (45), σ_T the relationship between temperature stress and constraint coefficient and other variables can be obtained as follows k_r:

$$\sigma_T = -k_r \alpha_T \Delta T . E\left(T_s\right). \tag{50}$$

In the equation,

$$k_r = 1 - \frac{\varepsilon_c}{\alpha_s \Delta T} = 1 - \frac{\Delta l}{\alpha_s \Delta T \cdot l_0} \tag{51}$$

where, is ε_c the actual strain of the cylindrical shell in the loading direction (axial direction); Δl is the actual deformation of the cylindrical shell, l_0 and is the original length of the cylindrical shell. ε_c It can be measured by a strain gauge, or the elongation Δl and original length l_0 of the cylindrical shell can be measured with a length measuring tool. Assuming that the constraint coefficient of the structure does not change during the temperature change process k_r, the constraint coefficient of the structure k_r can be obtained by simple calculation.

Appendix B

Numerical solution of stable bearing capacity of corroded thin plate

The wall thickness is taken as 2 mm, and the four-sided simply supported rectangular steel plate with a loaded side width of 60 mm is made of Q345 steel, which was corroded in Qingdao area. The temperature is approximately 293 K (20 °C). For a thin plate with a thickness of 2 mm, the uniform wiring pressure loads here are respectively taken as $p = 0$, $p = 150$ N/mm, and $p = 300$ N/mm. Based on the improved steel corrosion kinetics model, the change trend of the steel plate's stable bearing capacity with corrosion time can be obtained as shown in Fig. 4.

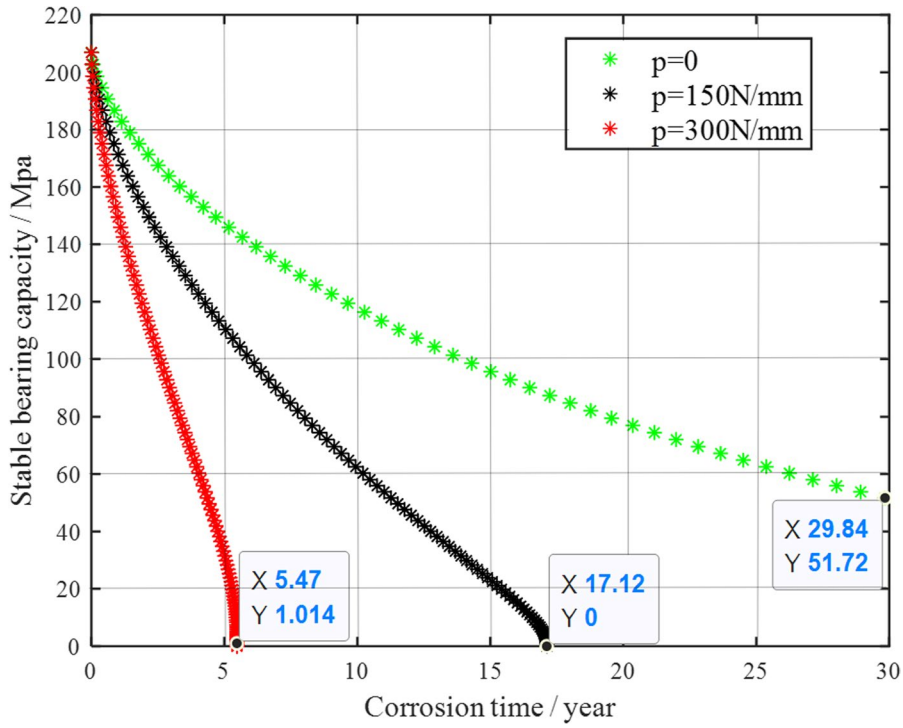

Fig. 4 Variation of stable bearing capacity of thin-walled steel plate with corrosion time under different loads

Figure 4 shows the variation of the stable bearing capacity of thin-walled steel plates with corrosion time under different loads. According to the small deflection stability theory of thin plates, the stable bearing capacity of thin-walled steel plates at the initial moment without corrosion can be obtained as:

$$\sigma_{cr} = \frac{\pi^2 E}{3(1-\mu^2)}\left(\frac{t}{b}\right)^2 = \frac{\pi^2 \times 206 \times 10^3 \text{Mpa}}{3(1-0.3^2)}\left(\frac{1\text{mm}}{60\text{mm}}\right)^2 = 206.87\ \text{MPa}\cdot$$

The results observed at the initial moment in Fig. 4 are consistent with it. As the corrosion time increases, the stable bearing capacity of the steel plate decreases rapidly, and the greater the external load, the faster the stable bearing capacity decreases.

Appendix C

Numerical solution of stable bearing capacity of corroded thin cylindrical shells

A simple-supported thin-walled steel cylindrical shell with a wall thickness of 2 mm and a radius of 400 mm (i.e., 0.4 m) at both ends is taken here, and the material is Q 345 steel. Corrosion occurs in the Qingdao area, and the temperature is approximately 293 K (20 °C). For a thin-walled cylindrical shell with a thickness of 2 mm, the uniform wiring pressure loads here are respectively taken as $p=0$, $p=100$ N/mm, and $p=200$ N/mm. Based on the improved steel corrosion kinetics model, the variation trend of the stable bearing capacity of thin-walled steel cylindrical shells with corrosion time can be obtained as shown in Fig. 5 below.

Figure 5 shows the large-deflection buckling critical stress of cylindrical shells changing with corrosion time under different loads. From the large-deflection stability theory of cylindrical thin shells, it can be obtained that the stable bearing capacity of cylindrical thin shells at the initial moment without corrosion is:

$$\sigma_{cr} = \frac{1}{3}\frac{1}{\sqrt{3(1-\mu^2)}}\frac{Eh}{r} = 0.605\frac{206\times10^3\text{Mpa}\times2\text{mm}}{400\text{mm}} = 207.79\ \text{MPa}\cdot$$

The results observed at the initial moment in Fig. 5 are consistent with it. With the increase of corrosion time, the stable bearing capacity of the thin steel cylindrical shell decreases rapidly, and the greater the external load, the faster the stable bearing capacity decreases.

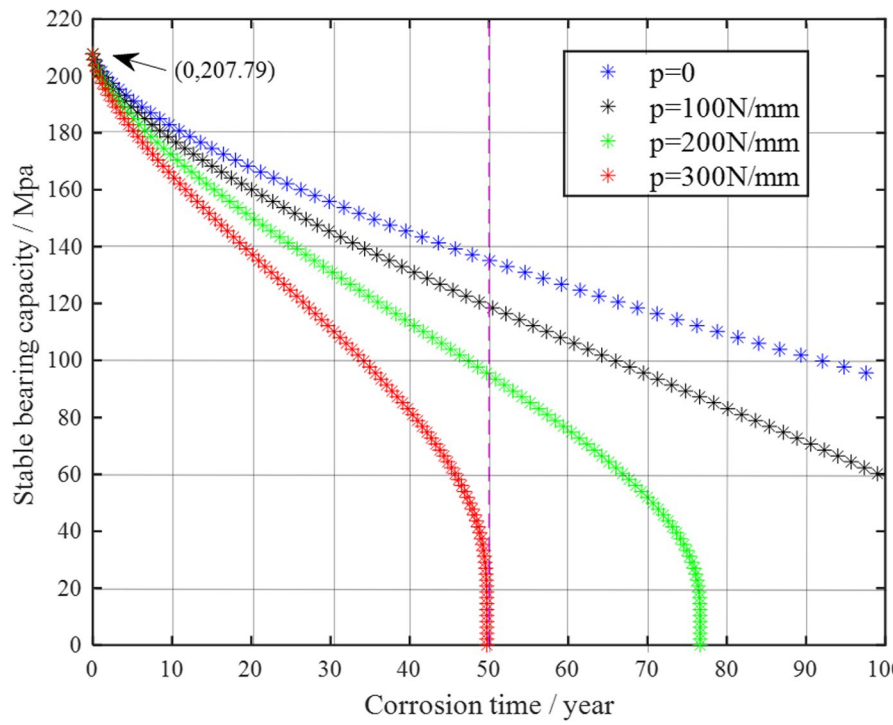

Fig. 5 Curves of large deflection buckling critical stress versus corrosion time for cylindrical shells under different loads

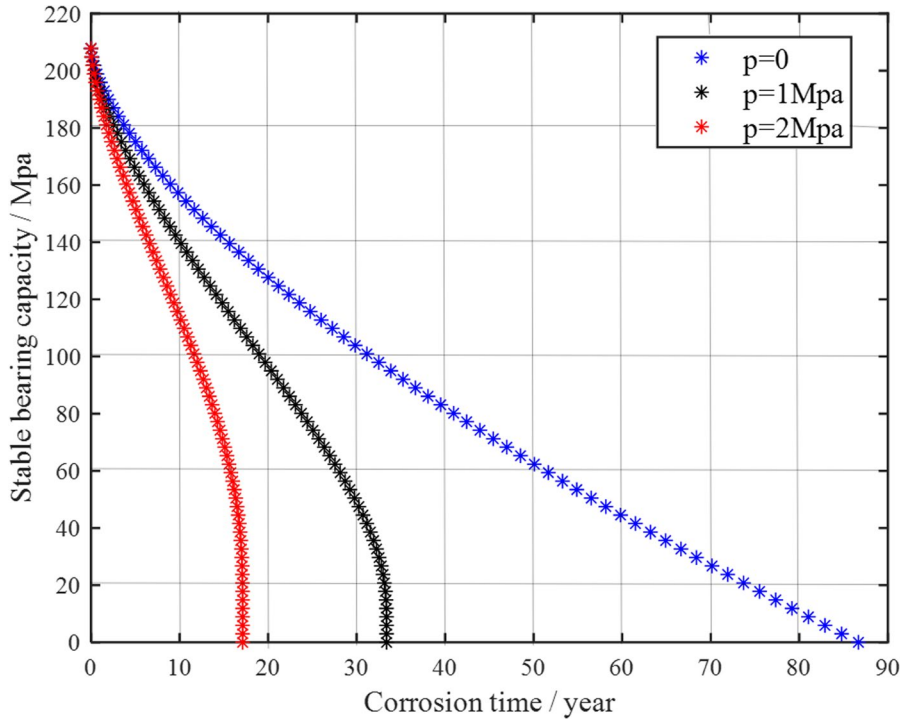

Fig. 6 Variation curve of stable bearing capacity of thin-walled spherical shell with corrosion time

Appendix D

Numerical solution of stable bearing capacity of corroded thin spherical shell

With thickness $h=1$ mm and radius $r=150$ mm is made of Q 345 steel. Corrosion occurs in Qingdao area, and the ambient temperature is approximately 20 °C (i.e., 293 K). For the uniformly distributed pressure load on the outer surface, three cases of $p=0$ MPa, $p=1$ MPa and $p=2$ MPa are considered respectively.

Figure 6 is the variation curve of the stable bearing capacity of the thin-walled spherical shell with corrosion time. From the large deflection stability theory of the thin-walled spherical shell, it can be obtained that the stable bearing capacity of the thin-walled spherical shell at the initial moment without corrosion is:

$$\sigma_{cr}=\frac{1}{4}\frac{1}{\sqrt{3(1-\mu^2)}}\frac{Eh}{r}=\frac{1}{4}\times 0.605\frac{206\times10^3\text{Mpa}\times2\text{mm}}{400\text{mm}}=207.79\text{ MPa}\cdot$$

The results observed at the initial moment in Fig. 6 are consistent with it. With the increase of corrosion time, the stable bearing capacity of the thin steel cylindrical shell decreases rapidly, and the greater the external load, the faster the stable bearing capacity decreases.

Appendix E

Numerical solution of stable bearing capacity of varying temperature corroded thin plates

The width of the loaded side of the thin-walled steel plate is $b=60$ mm, and the thickness of the plate is $h=2$ mm. The range of temperature variation is considered to be between 20 and 600 °C, and the restraint degree coefficients of the plates are selected as $k_r=0$ (free), $k_r=0.5$ (elastic restraint), and $k_r=1$ (fixed restraint). Neglect the change of constraint coefficient k_r in the process of temperature change, that is, assume that the constraint degree coefficient k_r does not change with temperature. Therefore, the variation law of the stable bearing capacity (critical stress) of the thin plate with the temperature of the steel plate can be drawn as shown in Fig. 7.

From Fig. 7 that under three different constraints, the stable bearing capacity of the thin-walled steel

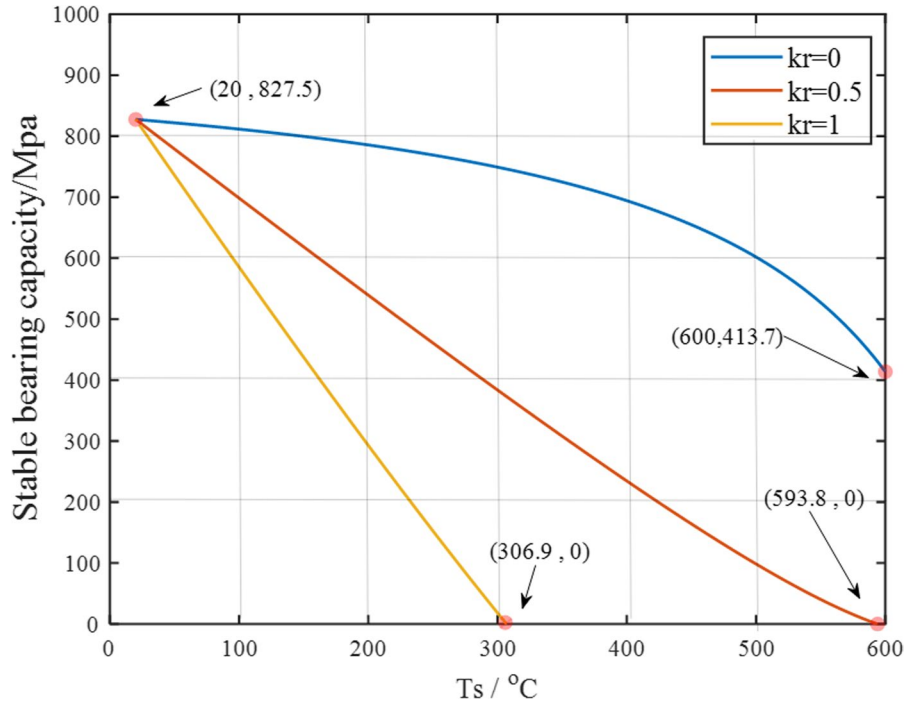

Fig. 7 Variation curves of stable bearing capacity of thin-walled steel plates with steel temperature for different degrees of restraint

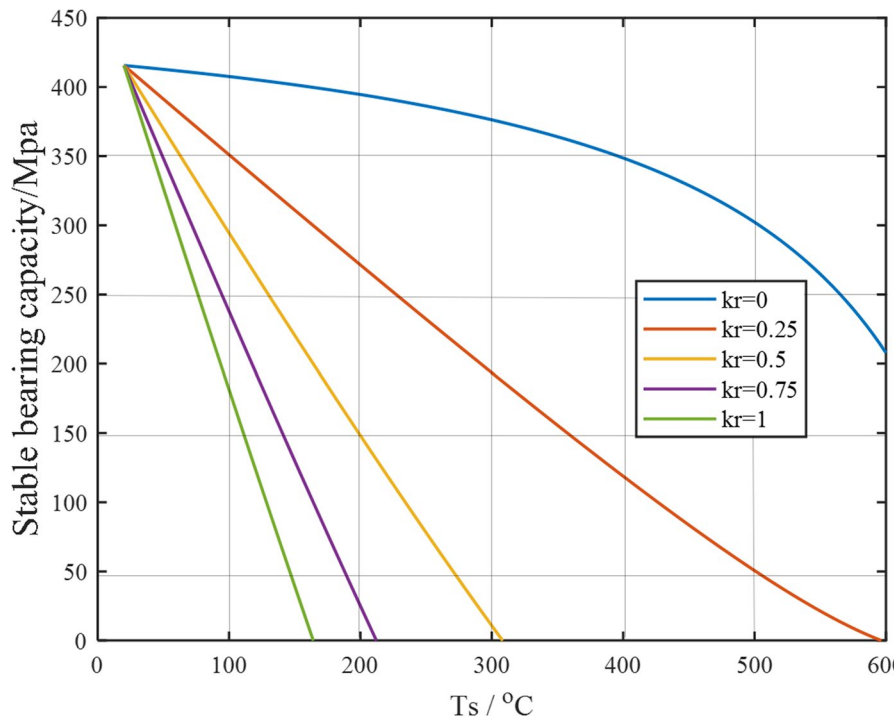

Fig. 8 Curves of the stable bearing capacity of thin steel cylindrical shells with different degrees of restraint as a function of steel temperature

plate decreases gradually with the increase of temperature.

Appendix F

Numerical solution of stable bearing capacity of thin cylindrical shell corroded by variable temperature

Thickness $h=4$ mm of thin-walled cylindrical steel shell, radius $r=400$ mm. Considering the range of temperature variation between 20 and 600 °C, the constraint degree coefficients at the end of the cylindrical shell are respectively $k_r=0$, $k_r=0.25$, $k_r=0.5$, $k_r=0.75$ and $k_r=1$. Neglect the change of constraint coefficient k_r in the process of temperature change, that is, assume that the constraint degree coefficient k_r does not change with temperature. Therefore, the critical stress of the thin-walled cylindrical steel shell (based on the large deflection stability theory) can be drawn as a function of the temperature of the steel shell as shown in Fig. 8.

From Fig. 8 that under the five different constraints, the stable bearing capacity of the thin-walled steel cylindrical shell decreases gradually with the increase of temperature. And the greater the degree of restraint, the faster the stable carrying capacity (as the temperature increases) decreases.

Appendix G

Numerical solution of stable bearing capacity of thin spherical shell corroded by variable temperature

Thickness of thin-walled steel spherical shell h = 4 mm, radius r = 400 mm. The range of temperature variation is considered between 20 and 600 °C. Regardless of the boundary constraints of the spherical shell, the critical stress (based on the large deflection stability theory) of the thin-walled steel spherical shell without boundary constraints can be drawn as a function of the temperature of the steel shell as shown in Figure.

Figure 9, when the temperature of the steel spherical shell with a thickness-to-diameter ratio of 1/100 rises from 20 to 600 °C, its stable bearing capacity drops from the initial 311.7–155.8 MPa, a drop of 50%. The decrease is exactly equal to the reduction of the elastic modulus of the structure at high temperature.

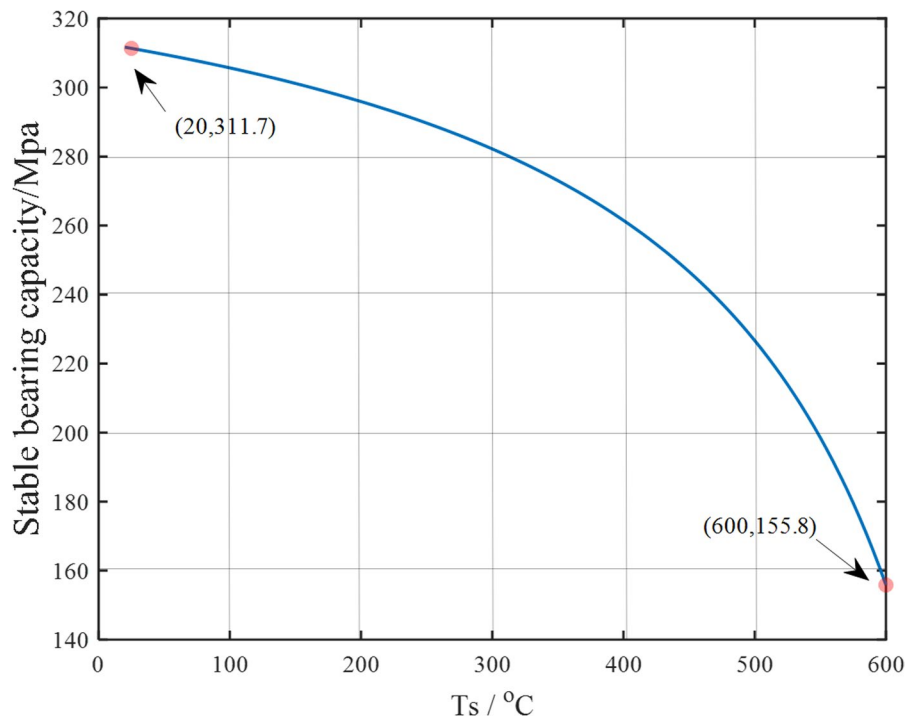

Fig. 9 Unconstrained Thin-walled Steel Spherical Shell Stable Bearing Capacity Variation Curve with Steel Temperature

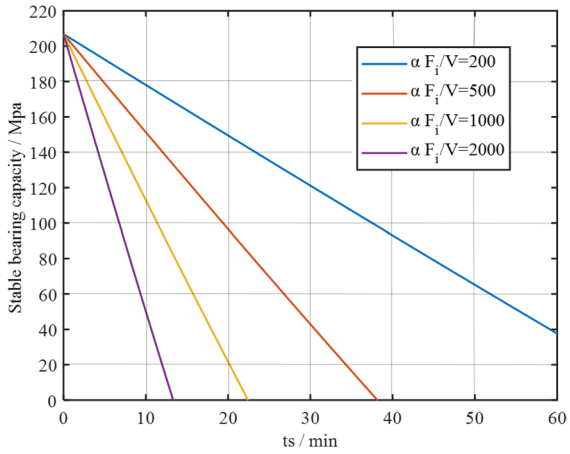

Fig. 10 H1 Stable bearing capacity of the thin plate as a function of fire duration

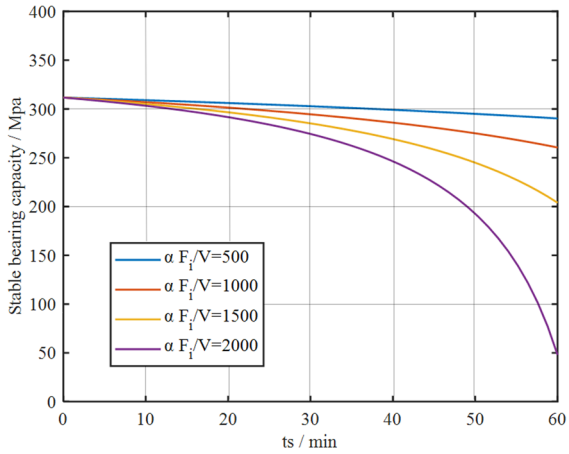

Fig. 11 Stable bearing capacity of thin cylindrical shells as a function of fire duration

Appendix H

Numerical solution of stable bearing capacity of fire corrosion thin plates

The steel plate has a width of 60 mm and a thickness of 1 mm. The elastic modulus of the steel is 206Gpa, the Poisson's ratio is 0.3, the boundary constraint degree coefficient of the thin plate is taken as $k_r = 0.5$, and the initial ambient temperature is 20 °C. Four different section shape coefficients are taken for analysis.

Figure 10 above shows the change of the stable bearing capacity of the thin plate with the fire duration under the fire temperature change. It can be seen from the figure that the greater the cross-sectional shape parameter of the thin plate, the faster the stability will be $\alpha F_i/V$ lost in the fire temperature change. The thin plate with section parameters $\alpha F_i/V$=2000(wall thickness h=1 mm) has completely lost its stable load-bearing capacity in less than 15 min.

Appendix I

Numerical solution of stable bearing capacity of thin cylindrical shells corroded by fire variations in temperature

The cylindrical thin shell has a radius of 400 mm and a wall thickness of 4 mm. The elastic modulus of the steel is 206 Gpa, Poisson's ratio is 0.3, the boundary restraint degree coefficient of the thin cylindrical shell is taken as $k_r = 0.5$, and the initial ambient temperature is 20 °C. Four different section shape coefficients are taken for analysis.

From Fig. 11 above, it can be seen that the larger the cross-sectional shape parameter of the thin cylindrical shell $\alpha F_i/V$, the faster it will lose stability in the fire temperature change. The cylindrical thin shell with section parameters $\alpha F_i/V = 2000$ (wall thickness h=4 mm) has completely lost its stable bearing capacity in less than 30 min.

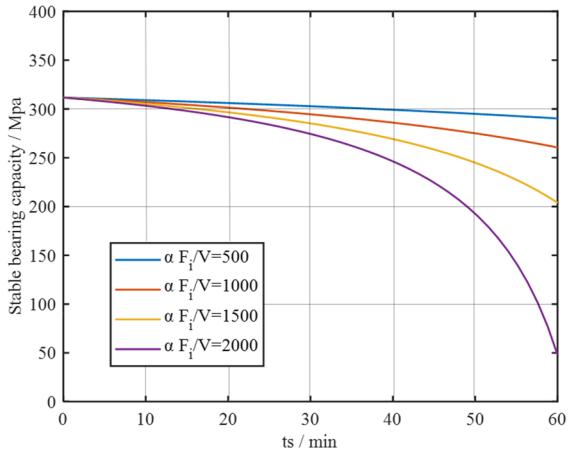

Fig. 12 The change of the stable bearing capacity of the unconfined spherical shell with the duration of the fire

Appendix J

Numerical solution of stable bearing capacity of thin cylindrical shells corroded by fire variations

The radius of the thin-walled spherical shell is 400 mm and the wall thickness is 4 mm. The modulus of elasticity of the steel is 2 06 Gpa and the Poisson's ratio is 0.3. The initial ambient temperature is 20 °C. Four different section shape coefficients are taken for analysis.

From the above Fig. 12, it can be seen that $\alpha F_i/V$ the larger the cross-sectional shape parameter of the thin-walled spherical shell, the faster the loss of stability in the fire temperature change, that is, the greater the decline in the stable bearing capacity within the same time period.

References

1. Gutman EM, Zainullin RS, Zaripov RA (1984) Kinetics of mechanical chemical failure and the life of constructional elements in tension in elastoplastic deformations. Soviet Mater Sci 20:101–103
2. Gutman EM, Haddad J, Bergman R (2005) Stability of thin-walled high-pressure cylindrical pipes with noncircular cross-section and variable wall thickness subjected to non-homogeneous corrosion. Thin-Walled Struct 43:23–32
3. WT Koiter (1945) The stability of elastic equilibrium. Thesis, Delft.
4. Sewell MJ (1965) The static perturbation technique in buckling problems. J Mech Phys Solids 13(4):247–265
5. Yuan H, Liu H, Ren X, Zhang X, Ai D, Luo Y (2019) The bearing performance of the bolt-sphere joints with stochastic pitting corrosion damage. J Constr Steel Res 160:359–373
6. Proserpio D, Ambati M, De Lorenzis L, Kiendl J (2021) Phase-field simulation of ductile fracture in shell structures. Comput Methods Appl Mech Eng 385:114019. https://doi.org/10.1016/j.cma.2021.114019
7. Hutchinson JW (2010) Knockdown factors for buckling of cylindrical and spherical shells subject to reduced biaxial membrane stress. Int J Solids Struct 47(10):1443–1448. https://doi.org/10.1016/j.ijsolstr.2010.02.009
8. Nemeth MP, Starnes JH (1998) The NASA monographs design recommendations a review on shell stability and suggested. Nasa/Tp-1998-206290
9. Wu L (1989) Plate-shell theory M. Shanghai Jiao Tong University Press, Shanghai
10. Fubao He, Yapeng S (1996) Plate-shell theory M. Huazhong University of Science and Technology Press, Wuhan
11. Gutman EM, Bergman RM, Levitsky SP (2016) Influence of internal uniform corrosion on stability loss of a thin-walled spherical shell subjected to external pressure. Corros Sci 111:212–215
12. Liu CH, Lacidogna GA (2023) Non-destructive method for predicting critical load, critical thickness and service life for corroded spherical shells under uniform external pressure based on NDT data. Appl Sci 13:4172–4191
13. Pronina YG (2015) Analytical solution for decelerated mechanochemical corrosion of pressurized elastic-perfectly plastic thick-walled spheres. Corros Sci 90:161–167
14. Pronina Y, Sedova O (2021) Analytical solution for the lifetime of a spherical shell of arbitrary thickness under the pressure of corrosive environments: the effect of thermal and elastic stresses. J Appl Mech Trans ASME. https://doi.org/10.1115/1.4050280
15. Wu L (1996) Plate and shell stability theory, 1st edn. Huazhong University of Science and Technology Press, Wuhan
16. Liang C, Hou W (1995) Eight-year atmospheric exposure corrosion research on carbon steel and low alloy steel. Corros Sci Prot Technol 7:65–73
17. Standard N (2018) Technical specifications for steel structures (GB 50017). China Architecture and Building Press, Beijing
18. Standard N (2013) Code for design of steel structures (GB50017-2003). China Planning Press, Beijing
19. Industry standard: Technical Code for Fire Protection of Building Steel Structures (GB51249-2017). China Planning Press, Beijing (2018)
20. Kang J, Zhao M, Jiang Y, Jing R (2014) Research on the relationship between degree of constraint and temperature stress. J Hydraul Archit Eng 12:21–25
21. Technical Code for Fire Protection of Building Steel Structures (GB51249-2017). Beijing China Planning Press, Beijing (2016).